Pressure-Induced Mott Transition Followed by a 24-K Superconducting Phase in $BaFe_2S_3$

Touru Yamauchi,[1] Yasuyuki Hirata,[1] Yutaka Ueda,[1,2] and Kenya Ohgushi[1,3]
[1]*Institute for Solid State Physics, University of Tokyo, 5-1-5 Kashiwanoha, Kashiwa, Chiba 277-8581, Japan*
[2]*Toyota Physical and Chemical Research Institute, 41-1 Yokomichi, Nagakute, Aichi 480-1192, Japan*
[3]*Department of Physics, Graduate School of Science, Tohoku University, 6-3, Aramaki Aza-Aoba, Aoba-ku, Sendai, Miyagi 980-8578, Japan*
(Received 24 July 2015; published 8 December 2015)

We performed high-pressure study for a Mott insulator $BaFe_2S_3$, by measuring dc resistivity and ac susceptibility up to 15 GPa. We found that the antiferromagnetic insulating state at the ambient pressure is transformed into a metallic state at the critical pressure, $P_c = 10$ GPa, and the superconductivity with the optimum $T_c = 24$ K emerges above P_c. Furthermore, we found that the metal-insulator transition (Mott transition) boundary terminates at a critical point around 10 GPa and 75 K. The obtained pressure-temperature (P-T) phase diagram is similar to those of the organic and fullerene compounds; namely, $BaFe_2S_3$ is the first inorganic superconductor in the vicinity of bandwidth control type Mott transition.

DOI: 10.1103/PhysRevLett.115.246402 PACS numbers: 71.30.+h, 74.62.Fj, 75.50.Dd

"Mott transition" has been an important keyword for modern physics for the last several decades, particularly since the discovery of high-T_c superconducting (SC) cuprates [1]. Many studies have been performed in wide classes of materials, from 3d-transition metal compounds to organic compounds which are expected to have a suitable ratio of U/t characterizing highly correlated electron systems, large Coulomb repulsion energy U, and small band width t [2]. In the case that a quantity U/t is large enough, the electrons should be localized, resulting in the Mott insulating state. Much work has been done to modify the Mott insulating state to the metallic one by substituting chemical elements and/or by applying pressure. These studies have revealed several kinds of electronic phase diagrams drawn as the function of temperature and some parameters (composition, pressure, and magnetic field) which control band filling and bandwidth, namely, U/t, and the type of Mott transition has also been argued, taking the orbital degeneracies and the geometry of lattice into account [3–5]. Typical examples of a bandwidth controlled-type phase diagram were observed in the layered organic conductors BEDT-TTF salts and the cation doped fullerene $A_3@C_{60}$ [6–9], in which the SC phases emerge incidental to the pressure-induced Mott transition. These pressure-temperature (P-T) phase diagrams of the half-filled Mott insulating compounds show good contrast to those observed in high-T_c SC cuprates as a function of chemical doping.

Meanwhile, there is a theoretical prediction that materials with the ladder-type crystal structure formed by transition metal ions are favorable for the SC state, when it turns metallic [10]. The title compound, $BaFe_2S_3$, is a possible candidate for such a ladder superconductor because of the following reasons: (i) The crystal structure shown in the inset of Fig. 1 can be regarded as a FeX (X = S, Se, As, P) square lattice, a crystallographically common feature of Fe-based superconductors [11–13], with stripe-ordered Fe ion vacancies. These Fe ion vacancies cut the square lattice, FeS, into ladders, Fe_2S_3, running along the c axis [14]. (ii) This compound is most conductive compared with other isostructural compounds such as $BaFe_2Se_3$ and $CsFe_2Se_3$ as characterized by thermal activated conductions with a smaller gap Δ [15–18]. (iii) This compound has a characteristic magnetic ground state, the stripe-type antiferromagnetic (AFM) state as

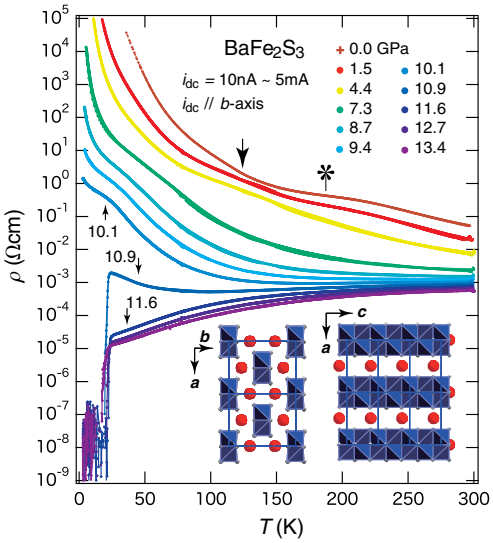

FIG. 1 (color online). The temperature dependences of dc resistivity (ρ-T curves) under constant pressures. The resistivity was measured along the c axis with several dc-excitation currents. The inset shows the crystal structure consisting of Fe_2S_3 ladders (blue polyhedra) and Ba ions (red balls).

frequently observed in Fe-based superconductors, and a small spin moment $m = 1.25\ \mu_B$ [19]. Note that the Fe ions are nominally divalent, Fe^{2+}: $(3d)^6$ electronic configurations in tetrahedral coordination in this compound. Therefore, $BaFe_2S_3$ has been a good target for metallization and superconductivity under high pressure. Actually, a recent work revealed that $BaFe_2S_3$ shows an appearance of the SC phase at $T_c \sim 14$ K under 11 GPa without major crystal structure change [19]. However, owing to the limitation of the hydrostaticity generated by the diamond anvil cell with the use of a solid pressure transmitting medium, the nature of Mott transition as well as the global phase diagram has not yet been unraveled.

In this work, we will present the results of the precise dc-resistivity and ac-susceptibility measurements using a cubic-anvil type pressure cell in which the liquid pressure transmitting medium is easy to be employed. Good hydrostatic pressure can avoid sample damage. We will show crucial evidences for the SC phase, both the zero-resistivity and clear shielding signals coming from the massive SC volume fraction. Furthermore, the dc-resistivity measurement reveals a typical P-T phase diagram expected for bandwidth control Mott transition as observed in BEDT-TTF salts and cation-doped fullerenes. The P-T phase diagram of $BaFe_2S_3$ will be totally discussed together with the magnetic and orbital ordering transitions observed at ambient pressure.

A multianvil type high-pressure cell equipped with sintered diamond anvils was employed for both dc-resistivity and ac-susceptibility measurements up to about 15 GPa. Glycerol was also employed as a pressure transmitting medium. The dc-resistivity measurements were performed by the standard four probes method with the several dc-excitation currents running along the c axis (leg direction). The ac susceptibility measurements were carried out using inductively coupled small coils in which both the sample crystal and the reference Pb metal were inserted as shown in the inset of Fig. 3. This experimental setting allows us to estimate the absolute value of SC volume fraction. The quality of sample crystals was crucial to observe the SC nature and was carefully checked by resistivity measurements at ambient pressure; namely, we chose the sample crystals that showed simple activation type conduction at low temperature [20].

Figure 1 exhibits the pressure evolution of the dc-resistivity temperature (ρ-T) curves observed at the several constant pressures as noted in this figure. The insulating nature at ambient pressure characterized by thermal activation-type conduction at low temperature is gradually suppressed as increasing pressure and the ρ-T curves under a few GPa become nonthermal activation type. When the resistivity at 300 K approaches the critical conductance at 10.1 GPa, $1/\rho \sim 0.03e^2/\hbar d$, where d is the Fe-Fe distance along the leg direction [21], the metallic nature emerges at around room temperature as observed in several kinds of pressure-induced metals [22]. Further compressing up to 10.9 GPa results in good metallicity of the system above 100 K and the ρ-T curve shows a moderate upturn below 80 K [23] followed by a sharp SC drop. All the ρ-T curves above the critical pressure, $P_c = 10.9$ GPa, clearly show the SC transition and reach to zero resistivity, as naturally expected from the bulk SC phase. Figure 2(a) shows all the ρ-T curves above 10.9 GPa in a linear plot. The onset and the offset temperatures of the SC transition at the optimum pressure, 11.6 GPa, are 24.6 and 22.6 K, respectively. Above 11.6 GPa, the ρ-T curves show Fermi-liquid-like T^2 behavior up to about 40 K. The A coefficient of the T^2 term is evaluated to be 16.1×10^{-9} Ωcm/K^2 at 11.6 GPa and 6.8×10^{-9} Ωcm/K^2 at 13.4 GPa.

Another important discovery in this work is that the phase boundary of the Mott transition exists and the boundary line has an end point in the pressure-temperature (P-T) phase diagram just like a gas-liquid phase boundary. Figure 2(b) presents the isothermal pressure dependences of resistivity (ρ-P curves) at several selected temperatures. These curves are obtained by picking up the isothermal data from ρ-T curves and by plotting them as a function of pressure. For easy viewing, each ρ-P curve is shifted

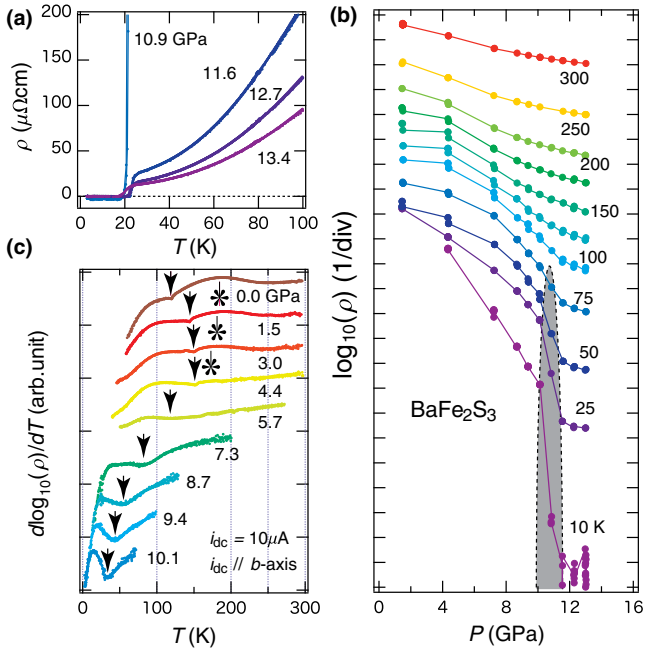

FIG. 2 (color online). (a) The ρ-T curves at 10.9, 11.6, 12.7, and 13.4 GPa in a linear plot, showing the zero resistivity due to the SC transition. (b) The isothermal pressure dependence of resistivity (ρ-P curves) in selected temperatures. For easy viewing, each the ρ-P curve is shifted with an arbitrary offset in the order of the temperatures. The hatched areas correspond to the metal-insulator transition boundary. (c) The temperature differentials of $\log_{10}(\rho)$ as functions of temperature below 10.1 GPa. These curves are shifted with an arbitrary offset in the order of the temperatures.

upward with an arbitrary offset in the order of the temperatures. Note that the vertical axis shows $\log_{10}(\rho)$, thus the change of 1 division in this figure means 10 times change of the ρ. The ρ-P curve at 10 K shows a huge drop at around $P_{\mathrm{Mott}} \sim 11$ GPa as a reflection of the phase transition from insulator to SC phase. In addition to this, the ρ-P curves at 25 and 50 K, wgich surely sit in the *non*-SC normal state, clearly show a stepwise decrease by an order of 10^{-4} (at 25 K) and 10^{-3} (at 50 K) at P_{Mott}. In contrast, the curves above 100 K show moderate decrease with increasing pressure without sudden change in the ρ. Note that P_{Mott} coincides with P_c within the experimental accuracy at the ground state. The region, in which the ρ shows a sudden decrease, is hatched by gray in Fig. 2(b). These features manifest the following two aspects: (i) There is a 1st order phase boundary between the Mott insulating and metallic states. (ii) This phase boundary has an end point at around 50–75 K.

The ρ-T curves give us further information. There are two phase transitions at ambient pressure; one is an AFM ordering and the other is possibly an orbital ordering (OO) transition [20,24,25]. These transitions can be seen as slight dimples (humps) on the ρ-T curves. Thus, the precise dc-resisitivity measurements are crucial to track the pressure evolutions of these transition temperatures (T_N and T_{OO}). The T_N and T_{OO} at 0.0 GPa (see Fig. 1) are marked by the arrow and asterisk, respectively. Since these anomalies are very small, it is hard to see them in the raw ρ-T curves. Accordingly, a set of temperature differentials of $\log_{10}(\rho)$ as a function of temperature is shown in Fig. 2(c), from which one can see the anomaly at T_N as dimples (arrows). Moreover, T_{OO} can be also observed as small humps on these curves (asterisk). The T_N increases from 122 K at 0.0 GPa to 150 K at 4.4 GPa, and then decreases above 4.4 GPa; meanwhile, the T_{OO} decreases monotonically with increasing pressure. The two transition temperatures seem to merge into one at around 4.4–5.7 GPa. These two transition temperatures become about 30 K just below P_{Mott}.

Generally, we cannot check the bulk character of the SC phase in dc-resisitivity measurement. In contrast, ac-susceptibility measurement is a good way to observe it. The pressure evolution of the ac susceptibility, that is the output signal of the receiver, versus temperature (V-T) curves is exhibited in the main panel of Fig. 3. Below 5 K, all the V-T curves show a SC transition signal (a stepwise drop) coming from the Pb reference sample as shown by a blue arrow on the 10.6 GPa curve. The SC transition temperature of Pb slightly decreases as increasing pressure, which is barely discernible in this figure. Using this transition temperature, we can estimate the actual pressure in the pressure cell, and the estimated pressures are noted near each V-T curve. At 9.8 GPa, a slight drop represented by a red arrow can be seen at 21.9 K, however, the SC signal is weak in consequence of the small SC volume fraction at this

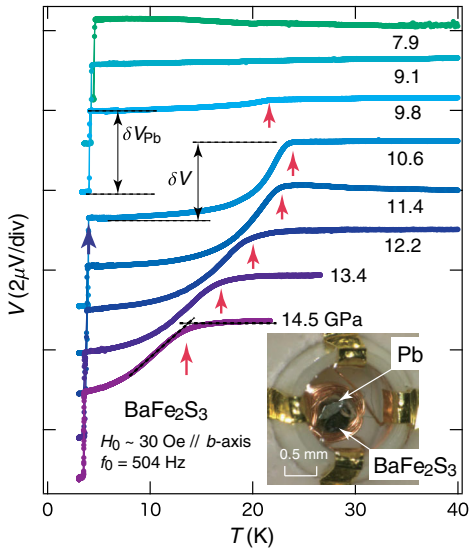

FIG. 3 (color online). The ac-susceptibility measurements under high pressure. The pressure evolution of the V-T curves (see main text) is observed up to 15 GPa by the ac excitation field $H_0 \sim 30$ Oe, the frequency $f_0 = 504$ Hz. Similar behavior was also observed in other frequencies ($f_0 = 52$ Hz, 5.1 kHz, data not shown). The magnitudes of the SC signals of both the sample and Pb reference, δV, δV_{Pb} are shown by vertical arrows. The sample setting in the coupled coils is shown in the inset, both the black sample crystal and the silver Pb reference can be seen.

pressure. A significant drop of the V-T curve appears at 23.8 K in the 10.6 GPa V-T curve. This is conclusive evidence for the bulky SC phase in $BaFe_2S_3$. The observed round shape has been frequently observed in the temperature dependence of susceptibility of type-II superconductors. Above 11.4 GPa, a clear pressure dependence of T_c can be seen. Note that the T_c is determined as a cross point of two broken lines as illustrated on the 14.5 GPa curve. By taking the SC signals of Pb reference into account, we can estimate the SC volume fraction and its pressure dependence. The magnitudes of SC signals of both $BaFe_2S_3$ and Pb, δV, and δV_{Pb} are defined as illustrated in the 10.6 and the 9.8 GPa curves, respectively. Considering that the ratio of the cross sections normal to the coil axis between the sample and the reference is 5:4 in this setting (inset of Fig. 3) and that Pb has a 100% SC volume fraction under pressure, we can estimate the SC volume fraction of the sample to be 80% at 10.6 GPa ($\delta V/\delta V_{\mathrm{Pb}} = 1.0$).

A P-T phase diagram is shown in Fig. 4(a). The results in both the dc-resistivity and ac-susceptibility measurements are represented as red and blue symbols in this figure, respectively. Note that there is small discrepancy between the pressures estimated in these two kinds of measurements because of the experimental limitation. Actually, the P_c's in these measurements differ from each other ($P_c = 10.9$ and 9.8 GPa in dc ρ and ac χ, respectively). A significant aspect of this phase diagram is that pressure of 15 GPa can tune the ground state of $BaFe_2S_3$ from AFM Mott insulating to

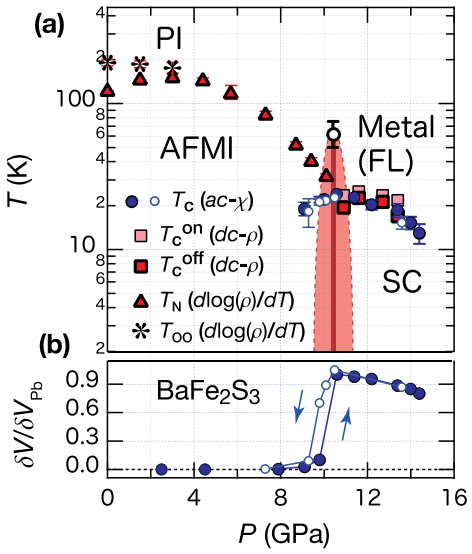

FIG. 4 (color online). (a) The pressure-temperature (P-T) phase diagram elucidated from both the dc-resistivity (red) and ac-susceptibility (blue) measurements. The T_{OO}, T_N, and T_c stand for the orbital ordering (OO), antiferromagnetic (AFM) ordering, and superconducting (SC) transition temperatures, respectively. The Mott transition shown in Fig. 2(b) is represented by the bold vertical line. "AFMI," "PI," "SC," and "FL" are abbreviations for the AFM Mott insulator, paramagnetic Mott insulator, SC, Fermi liquid phases, respectively. (b) The pressure dependence of the SC volume fraction [filled (open) symbols show P-increasing (decreasing) processes] at around 4 K derived from the ac-susceptibility measurement.

the bulk SC phase. This SC phase has a domelike shape with the optimum T_c of 24 K, adjacent to the Mott transition phase boundary shown by a bold vertical line with a shadowed area in Fig. 4(a). This Mott transition boundary at around 11 GPa has an end point at 50–75 K. At higher pressure, T_c gradually decreases down to 13 K at 14.5 GPa, which is almost half of the optimum T_c; in this course, the SC volume fraction moderately decreases from 80% to 64%. These aspects show the stable nature of the SC phase even at higher pressure. Moreover, the pressure dependence of the SC volume fraction shows a clear hysteresis as shown in Fig. 4(b). This feature reveals the 1st order nature of the transition between the superconducting and insulating phases. Additionally, the pressure evolutions of T_N and T_{OO} are also exhibited by the symbols of triangle and asterisk in this diagram, respectively. Even though the natures of these two transitions are not clear, owing to a lack of microscopic investigations, these pressure dependences are meaningful, because the temperature scales of both the T_N and the T_c are similar at P_c and/or P_{Mott}.

The current compound $BaFe_2S_3$ is considered to be a lower-dimensional version of Fe-based superconductors, which share the FeX (X = Se, P, As) square lattice as a structural motif. This reminds us of the relationship between $Sr_2Ca_{12}Cu_{24}O_{41}$ with the Cu ladder lattice and most of the high-T_c SC cuprates with the Cu square lattice. Interestingly, both the SC phases in $BaFe_2S_3$ and $Sr_2Ca_{12}Cu_{24}O_{41}$ appear only under pressure [26]. Naively, these observations lead us to image the similar P-T diagrams; however, these compounds have quite different underlying physics [27]. In $Sr_2Ca_{12}Cu_{24}O_{41}$, it is known that charge is transferred from the Cu chain to the Cu ladder sites by substituting isovalent Ca ion into Sr sites and/or applying pressure [28]. Contrary to this, in $BaFe_2S_3$, such filling control cannot be expected because of the single Fe site; hence, the Mott transition in $BaFe_2S_3$ is categorized to the bandwidth control type. Indeed, our observed P-T phase diagram is similar to that observed in the bandwidth control type Mott transition systems, quasi-2D organic compounds (BEDT-TTF salts), even though the pressure scale in this study (~10 GPa) is significantly higher than that in the organic conductors (~1 GPa). In BEDT-TTF salts, which are half-filled typical Mott insulators at ambient pressure, the Mott gap collapses at the critical pressures, culminating in the SC phases; the gap collapse is clearly observed as a relatively large jump of ρ, and the phase boundary line between Mott insulator and Fermi liquid lies almost vertical, more precisely it has slight positive or negative slope, and has an end point at the finite temperature in the P-T diagram [6]. The slope of the boundary line has been discussed in terms of spin entropy differences between metallic and Mott-insulating phases [7,8]. Those situations are quite similar to our observations in $BaFe_2S_3$, although it is unclear whether the phase boundary line has a slight slope or not. To obtain a further precise P-T diagram of $BaFe_2S_3$, in which the precise phase boundary and the position of the end point can be seen, significant improvements of high-pressure experimental technique are desirable.

There are two important aspects when the ideal Mott gap is closed by the bandwidth control. One is that the transition is 1st order, and the other is that the transition is accompanied with *no* symmetry change. In the case of $BaFe_2S_3$, both the criteria seem to be confirmed as follows: (i) The ρ-P curve at 25 K just above T_c shows a huge change at around P_{Mott} and the pressure dependence of the SC volume fraction has a clear hysteresis. These facts suggest the 1st order transition. (ii) The gap closing phase boundary seems to be terminated at the end point. If there is any symmetry change contrary to the ideal bandwidth control type Mott transition, *no* end point on the boundary is allowed. Therefore, these aspects strongly suggest that $BaFe_2S_3$ is the first inorganic Mott insulator in which pressure (bandwidth tuning) can suppress the Mott gap and make the ground state a SC phase. In addition, the orbital degree of freedom that is expected in Fe based compounds [29] is a significant difference between $BaFe_2S_3$ and the organic SC conductors.

The authors thank Professor H. Takahashi, Dr. K. Matsubayashi, Professor Y. Uwatoko, Professor M. Takigawa, and Professor K. Kindo for fruitful discussions. T. Y. also thanks Professor H. Ueda for developments and instructions of the automated cubic-anvil-type high-pressure cell system named "Oshitaro". This study was supported by the Grant-in-Aid for Scientific Research (No. 18104008) from the Japan Society for the Promotion of Science and the Grant Program of the Yamada Science Foundation.

[1] P. A. Lee, N. Nagaosa, and X-G. Wen, Rev. Mod. Phys. **78**, 17 (2006).
[2] M. Imada, A. Fujimori, and Y. Tokura, Rev. Mod. Phys. **70**, 1039 (1998).
[3] One can find many kinds of phase diagrams concerning Mott transitions in Ref [2]. The phase diagrams, for instance, in $R\mathrm{NiO}_3$, $\mathrm{V}_2\mathrm{O}_3$, and $R_{1-x}A_x\mathrm{VO}_3$ with both the filling and bandwidth tuning parameters are well known. These systems have been discussed taking the orbital degeneracy into account.
[4] K. Kanoda and R. Kato, Annu. Rev. Condens Matter Phys. **2**, 167 (2011).
[5] T. Mizusaki and M. Imada, Phys. Rev. B **74**, 014421 (2006).
[6] S. Lefebvre, P. Wzietek, S. Brown, C. Bourbonnais, D. Jérome, C. Mézière, M. Fourmigué, and P. Batail, Phys. Rev. Lett. **85**, 5420 (2000).
[7] F. Kagawa, T. Itou, K. Miyagawa, and K. Kanoda, Phys. Rev. B **69**, 064511 (2004).
[8] Y. Kurosaki, Y. Shimizu, K. Miyagawa, K. Kanoda, and G. Saito, Phys. Rev. Lett. **95**, 177001 (2005).
[9] Y. Takabayashi, A. Y. Ganin, P. Jeglič, D. Arčon, T. Takano, Y. Iwasa, Y. Ohishi, M. Takata, N. Takeshita, K. Prassides, and M. J. Rosseinsky, Science **323**, 1585 (2009).
[10] E. Dagotto and T. M. Rice, Science **271**, 618 (1996).
[11] Y. Kamihara, H. Hiramatsu, M. Hirano, R. Kawamura, H. Yanagi, T. Kamiya, and H. Hosono, J. Am. Chem. Soc. **128**, 10012 (2006).
[12] P. Dai, J. Hu, and E. Dagotto, Nat. Phys. **8**, 709 (2012).
[13] N. L. Wang, H. Hosono, and P. Dai, *Iron-Based Superconductors: Materials, Properties and Mechanisms* (Taylor & Francis, London, New York, 2012).
[14] E. Dagotto, Rev. Mod. Phys. **85**, 849 (2013).
[15] J. M. Caron, J. R. Neilson, D. C. Miller, A. Llobet, and T. M. McQueen, Phys. Rev. B **84**, 180409R (2011).
[16] H. C. Lei, H. Ryu, A. I. Frenkel, and C. Petrovic, Phys. Rev. B **84**, 214511 (2011).
[17] Y. Nambu, K. Ohgushi, S. Suzuki, Fei Du, M. Avdeev, Y. Uwatoko, K. Munakata, H. Fukazawa, S. Chi, Y. Ueda, and T. J. Sato, Phys. Rev. B **85**, 064413 (2012).
[18] F. Du, K. Ohgushi, Y. Nambu, T. Kawakami, M. Avdeev, Y. Hirata, Y. Watanabe, T. J. Sato, and Y. Ueda, Phys. Rev. B **85**, 214436 (2012).
[19] H. Takahashi, A. Sugimoto, Y. Nambu, T. Yamauchi, Y. Hirata, T. Kawakami, M. Avdeev, K. Matsubayashi, F. Du, C. Kawashima, H. Soeda, S. Nakano, Y. Uwatoko, Y. Ueda, T. J. Sato, and K. Ohgushi, Nat. Mater. **14**, 1008 (2015).
[20] Y. Hirata, S. Maki, J. I. Yamaura, T. Yamauchi, and K. Ohgushi, Phys. Rev. B **92**, 205109 (2015).
[21] N. F. Mott, *Metal-insulator transitions*: 2nd ed. (Taylor & Francis, London, New York, 1990), p. 46.
[22] T. Yamauchi and Y. Ueda, Phys. Rev. B **77**, 104529 (2008).
[23] This moderate upturn of the ρ-T curve shows stronger localization than the weak localization such as log-T (2D) and $T^{-1/2}$ (1D) behaviors. This is probably attributed to the fact that the 10.9 GPa ρ-T curve was measured almost along the Mott transition boundary line.
[24] T. Shimojima, K. Ishizaka, Y. Ishida, N. Katayama, K. Ohgushi, T. Kiss, M. Okawa, T. Togashi, X. Y. Wang, C. T. Chen, S. Watanabe, R. Kadota, T. Oguchi, A. Chainani, and S. Shin, Phys. Rev. Lett. **104**, 057002 (2010).
[25] S. Ishida, M. Nakajima, T. Liang, K. Kihou, C. H. Lee, A. Iyo, H. Eisaki, T. Kakeshita, Y. Tomioka, T. Ito, and S. Uchida, Phys. Rev. Lett. **110**, 207001 (2013).
[26] M. Uehara, T. Nagata, J. Akimitsu, H. Takahashi, N. Môri, and K. Kinoshita, J. Phys. Soc. Jpn. **65**, 2764 (1996).
[27] This is probably due to the crystallographic difference between $\mathrm{BaFe}_2\mathrm{S}_3$ and $\mathrm{Sr}_2\mathrm{Ca}_{12}\mathrm{Cu}_{24}\mathrm{O}_{41}$. Fe ions sit at a single site in contrast to the multiple Cu sites. These multiple sites allow the Cu ions to have a charge degree of freedom. This situation is probably crucial for the difference of the P-T phase diagrams.
[28] T. Osafune, N. Motoyama, H. Eisaki, and S. Uchida, Phys. Rev. Lett. **78**, 1980 (1997).
[29] T. Misawa and M. Imada, Nat. Commun. **5**, 5738 (2014).